Revisiting amorphous molybdenum sulfide's activity for the electro-driven reduction of dinitrogen and N-containing substrates

Kun Yang, Matthieu Koepf, Vincent Artero

▶ **To cite this version:**

Kun Yang, Matthieu Koepf, Vincent Artero. Revisiting amorphous molybdenum sulfide's activity for the electro-driven reduction of dinitrogen and N-containing substrates. Chemical Communications, 2020, 56 (90), pp.13975-13978. 10.1039/d0cc05078d . hal-03087266

HAL Id: hal-03087266
https://hal.science/hal-03087266

Submitted on 18 Oct 2022

HAL is a multi-disciplinary open access archive for the deposit and dissemination of scientific research documents, whether they are published or not. The documents may come from teaching and research institutions in France or abroad, or from public or private research centers.

L'archive ouverte pluridisciplinaire **HAL**, est destinée au dépôt et à la diffusion de documents scientifiques de niveau recherche, publiés ou non, émanant des établissements d'enseignement et de recherche français ou étrangers, des laboratoires publics ou privés.

COMMUNICATION

Revisiting amorphous molybdenum sulfide's activity for the electro-driven reduction of dinitrogen and N-containing substrates

Received 00th January 20xx,
Accepted 00th January 20xx

DOI: 10.1039/x0xx00000x

Kun Yang,[a] Matthieu Koepf,*[a] and Vincent Artero*[a]

Ammonia (NH_3) is a major feedstock of the chemical industry. The imperious need to decarbonize its production stimulated the quest for efficient catalysts able to drive the direct electro-reduction of dinitrogen (N_2) into NH_3. A large number of materials have now been proposed for this reaction, including bioinspired molybdenum sulfide derivatives. Here we revisit the potential of amorphous molybdenum sulfide to drive the electrocatalytic reduction of N_2 and other substrates of the nitrogenase. We find that this material exhibits negligible activity towards N_2 but achieves efficient reduction of inorganic azides.

Over the course of evolution, diazotrophic organisms have selected a specialized family of enzymes *i.e* the nitrogenases that are able to reduce dinitrogen (N_2) to ammonia (NH_3) via multiple electron and proton transfer under physiological conditions. The reaction occurs at highly preserved (hetero)metal sulfide cofactors such as the FeMoCo.[1,2] Synthetic transition metal sulfides can be viewed as analogues of these cofactors and are appealing candidates for developing catalysts for the electro-driven N_2 reduction reaction (NRR).[3] Iron and molybdenum derivatives have been particularly scrutinized as the latter metals are involved in the FeMoCo which supports the most active form of the enzyme.[1] Early examples of synthetic mimics incorporating these transition metals were indeed reported to exhibit some activity towards N_2 reduction.[4–6] Recent theoretical studies emphasized the potential of molybdenum sulfide derivatives for NRR,[7–9] which was quickly confirmed experimentally.[10–15] Meanwhile, several other families of metal-sulfide have been tested and showed promising results for the electrocatalytic reduciotn of N_2.[16–18] The reported activity of crystalline MoS_2 towards NRR in aqueous conditions, strongly arouse our curiosity since our group has been involved in the study of related catalytic materials for photo- and electro-driven proton reduction over the last years.[19–21] Specifically, the reports of X. Sun *et al*.[11] and Lou and *al*.,[13] highlighting enhanced NRR performances of defect-rich crystalline MoS_2 derivatives when compared to their defect-free counterparts, prompted us to investigate the potential of amorphous molybdenum sulfide (*a*-MoS_x) for electro-driven N_2 reduction.

Lacking long-range crystalline order, *a*-MoS_x is composed of chains of trigonal molybdenum $\{Mo_3S_7\}$ and $\{Mo_3S_6\}$ clusters connected via shared disulfide ligands.[21,22] It has demonstrated superior activity for proton reduction when compared to crystalline MoS_2, due to the increased accessibility of the Mo centers of the individual clusters after partial elimination of the terminal disulfide ligands under reductive conditions.[21,22] It is tempting to compare the resulting unsaturated Mo sites to the "surface defects" of crystalline MoS_2, thus, *a*-MoS_x appeared to us as an ideal candidate for promoting NRR. To probe this hypothesis we adapted classical conditions from the literature and investigated the potential of this material for driving N_2 reduction in aqueous conditions.

Thin films of *a*-MoS_x particles were deposited with or without Nafion ionomer onto 1 cm^2 glassy carbon electrodes (loading: 0.3 $mg_{a\text{-}MoSx}.cm^{-2}$). The latter were used as working electrodes (WE) in a classical three electrodes configuration, for over 20 h-long potential-controlled electrolysis in N_2-saturated aqueous electrolytes. Unless otherwise indicated, during the electrolysis the WE was polarized at a –0.3 V *vs*. the reversible hydrogen electrode (RHE) in 10 mL of the selected electrolyte, and aliquots were taken at fixed times for analysis. The concentration of ammonia in these samples was determined using the salicylate colorimetric method.[23] Due to the instability of *a*-MoS_x particles in solutions of pH ≥ 7 for long electrolysis times, we used either 0.1 M HCl (pH = 1) or 0.1 M potassium phosphate buffer (KPi, pH = 5.8) as electrolytes. During the electrolysis, N_2 was continuously fed into the electrolyte at a rate of 10 $mL.min^{-1}$. The NRR measurements were completed with a set of 5 control experiments (Table 1) allowing to define

[a] *Univ. Grenoble Alpes, CNRS, CEA, IRIG, Laboratoire de Chimie et Biologie des Métaux, 38000 Grenoble, France.*
E-mail: matthieu.koepf@cea.fr; vincent.artero@cea.fr

Electronic Supplementary Information (ESI) available: detailed experimental and data analysis procedures, additional statistical analysis and raw data for all experiments, TON and TOF calculations details. See DOI: 10.1039/x0xx00000x

Please do not adjust margins

Table 1: Experimental conditions used for control (HCl-1/KPi-1 – HCl-5/KPi-5) and NRR (HCl-6/KPi-6, HCl-7/KPi-7) experiments, in 0.1 M HCl and 0.1 M KPi (pH = 5.8) solutions.

Series	*α*-MoS_x ($mg.cm^{-2}$)	Nafion	Bias (*vs.* RHE)	Gas	Time (h)
HCl-1 / KPi-1	n.a[a]	n.a[a]	n.a[a]	N_2	>20
HCl-2 / KPi-2	0	–	–0.3	N_2	>20
HCl-3 / KPi-3	0	+	–0.3	N_2	>20
HCl-4 / KPi-4	0.3	+	O.C.P[b]	N_2	>20
HCl-5 / KPi-5	0.3	+	–0.3	Ar	>20
HCl-6 / KPi-6	0.3	–	–0.3	N_2	>20
HCl-7 / KPi-7	0.3	+	–0.3	N_2	> 20

[a] direct purge, no electrodes/electrochemical set up involved. [b] open circuit potential: complete three electrode setup without connecting the potentiostat.

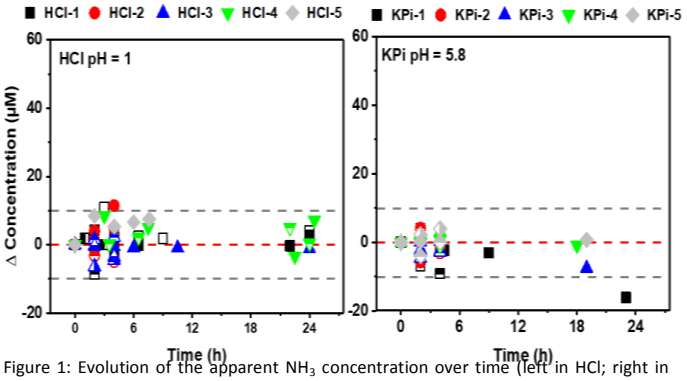

Figure 1: Evolution of the apparent NH_3 concentration over time (left in HCl; right in KPi) for all control groups. The distinct filling patterns within each series indicates measurements executed on samples collected from independent runs.

the background concentration of adventitious ammonia inherent to our experimental conditions. All the experiments (control and NRR) were conducted at least two times to build the datasets discussed in the following.

Due to the overall low concentration of NH_3 typically measured in these experiments, small variations of the concentration of adventitious ammonia can significantly affect the absorbance of the samples in the salicylate assay, even at time zero (t = 0) where virtually no ammonia is expected (ESI, Figure S2). Because the apparent 'zero' ammonia concentration measured for each experimental series appears random and never null, all the datasets discussed below are corrected for the absorbance at t = 0 for each series. Negative concentrations, thus, indicate a decrease of the apparent ammonia concentration in the electrolyte relative to t = 0. Furthermore, during the course of the electrolysis, the total volume of electrolyte decreases due to the sampling. This induces an overestimation of any variation of the apparent ammonia concentration between successive measurements. To compensate for this effect we corrected all the data reported in the following as explained in the ESI.

First, let us consider the evolution of the ammonia concentration measured over time for the control series HCl-1/KPi-1 – HCl-5/KPi-5 (Figure 1; ESI, Figure S8a-j). No strong trends appear in any series. We observe a random distribution of the concentrations with respect to time zero with equal chances of measuring an increase or a decrease of the apparent ammonia concentration over time in both 0.1 M HCl and 0.1 M KPi, as illustrated by the frequency distribution histograms (ESI, Figure S9). Overall more than 95% of the experimental values remain within ± 10 µM of the initial ammonia concentration for up to 25 hours in all the series (ESI, Table S3). In the following, thus, any variation of the ammonia concentration falling within this range will be considered as mere fluctuation of the experimental background concentration of adventitious NH_3.

We next turned to controlled electrolysis experiments run in N_2-saturated electrolyte over *α*-MoS_x thin-films (series HCl-6/KPi-6 and HCl-7/KPi-7, Figure 2). Here again, the concentration of ammonia measured in both 0.1 M HCl and 0.1 M KPi electrolyte remains generally close to the range of the experimental background. Furthermore, no traces of hydrazine could be detected in the electrolyte using the method of Watt and Chrisp (detection limit 5 µM),[24] in any of the conditions tested. Therefore, *α*-MoS_x does not exhibit the expected activity towards direct electro-driven N_2 reduction.

A more detailed analysis of the series is, however, interesting. Controlled electrolysis run on Nafionless films in both electrolytes (series HCl-6, KPi-6) as well as controlled electrolysis conducted over Nafion-containing films in 0.1 M HCl (series HCl-7) lead to an essentially random evolution of the ammonia concentration over time. The dispersion of the individual values remains strictly within the range of the experimental background and *α*-MoS_x is clearly inactive for NRR in these conditions. Surprisingly a small but steady increase in the ammonia concentration is, however, observed during the controlled electrolysis run in N_2-saturated 0.1 M KPi, on films incorporating Nafion (series KPi-7). The overall quantity of NH_3 released appears slightly dependent on the bias applied, with slightly higher NH_3 concentrations reached after long electrolysis run at –0.3V *vs*. RHE (ESI, Figure S10). In addition, we note a clear correlation between the quantity of ammonia detected in the electrolyte and the total charge passed during the electrolysis for KPi-7 series, in strong contrast with HCl-7, as shown on Figure S11 (ESI). These observations suggest that Nafion-coated *α*-MoS_x promotes a sluggish electro-driven release of ammonia in 0.1 M KPi under N_2. In order to probe whether traces amount of nitrite (NO_2^-) or nitrate (NO_3^-) resulting from the hydration of NO_x impurities present in the feeding gas may be the source of ammonia detected in our experiments,[25] we determined their concentration using the Griess assay.[27] As shown in Table S6 (ESI), the variation of the concentration of both anions remained under the detection limit of the assays (~ 1 µM) in 0.1 M KPi buffer under constant N_2 feeding (10 $mL.min^{-1}$) for at least 24 h. The accumulation of NH_3 observed for KPi-7 series, thus, likely originates from another source of nitrogen, however, we cannot exclude the direct reduction of neutral NO_x contaminants on *α*-MoS_x.[27] Additional experiments, such

This journal is © The Royal Society of Chemistry 20xx

Please do not adjust margins

Please do not adjust margins

as ^{15}N labeling, are needed to identify the source of NH_3 with certainty. Nevertheless, even when assuming direct NRR for series KPi-7, it should be noted that the mean rate of ammonia production in our experiments (0.070 ± 0.005 $\mu mol_{NH3}.h^{-1}.mg_{\alpha\text{-}MoSx}^{-1}$) is more than one order of magnitude lower than values typically reported for molybdenum sulfide based materials (0.1 to 4.1 $\mu mol_{NH3}.h^{-1}.mg_{cat}^{-1}$; ESI, Table S1). The contrast is really striking with respect to the rates reported for defect-rich MoS_2 (1.7 $\mu mol_{NH3}.h^{-1}mg_{MoS2}^{-1}$; in 0.1 M Na_2SO_4 at –0.4 V vs. RHE),[11] and amorphous MoS_3 (3 $\mu mol_{NH3}.h^{-1}.mg_{MoS3}^{-1}$; in 0.5 M $LiClO_4$ at –0.3 V *vs*. RHE) recently described by Liu *et al.*[14] The different nature of the electrolytes may partly explain these observations, however, the magnitude of the difference between the rates of ammonia production determined for *a*-MoS_x and those reported for defect-rich MoS_2 or amorphous MoS_3 is surprisingly large for related forms of molybdenum sulfide. The comparison with amorphous MoS_3 is particularly relevant. In-depth spectroscopic investigations of MoS_3 films prepared in a similar manner as described by Liu et *al*., strongly suggested that the latter is also composed of chains of interconnected trigonal $\{Mo_3S_x\}$ clusters.[28] Thus, MoS_3 and *a*-MoS_x are likely closely-related forms of molybdenum sulfide. In fact, noticeable differences between the rates of ammonia production reported for supposedly identical forms of molybdenum sulfide catalysts are found through the literature (ESI, Table S1). Considering the issues recently raised for other families of catalysts,[25,27] a careful re-evaluation of the activity of molybdenum sulfides for NRR appears timely to rationalize the apparent discrepancy found between studies.

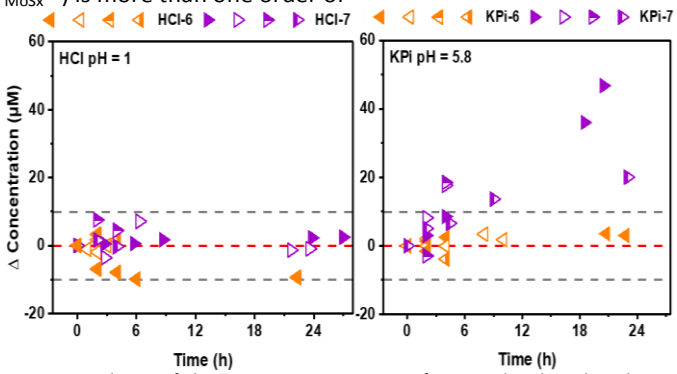

Figure 2: Evolution of the apparent concentration of NH_3 in the electrolyte during potential-controlled electrolysis in N_2-saturated 0.1 M HCl (left) or 0.1 M KPi buffer (pH = 5.8, right) using bare (HCl-6/KPi-6) or Nafion-coated (HCl-7/KPi-7) *a*-MoS_x films deposited on glassy carbon electrodes. The working electrode was polarized at -0.3 V *vs*. RHE. The distinct filling patterns within each series indicates measurements executed on samples collected during independent runs.

Next, we investigated the activity of *a*-MoS_x towards other N-containing substrates of the nitrogenases leading to the release of ammonia under (non-physiological) turnover conditions: hydrazine (N_2H_4), hydroxylamine (NH_2OH), nitrate (NO_3^-), nitrite (NO_2^-), and azide (N_3^-).[1,29] The electro-reduction of these substrates was first tested under potential-controlled electrolysis on pristine *a*-MoS_x films, in argon-saturated 0.1 M KPi electrolyte (pH = 5.8) with an applied potential of –0.2 V *vs*. RHE (ESI; Figure S12). During the initial screening, only hydroxylamine and azide resulted in a clear accumulation of ammonia in the electrolyte. From cyclic voltammetry measurements, the onset potentials of the catalytic processes can be estimated at 0.38 V and 0.36 V *vs*. RHE for NH_2OH and N_3^- respectively (ESI; Figure S13). Unfortunately, NH_2OH interfered with both the salicylate assay and selective ammonia electrode measurements, impeding the accurate quantification of NH_3 produced during the electrolysis. Such issues were not faced with azide, which allowed us to investigate the activity of *a*-MoS_x for its reduction in more details. A significant and steady increase in the concentration of ammonia is observed during the electrolysis of a 10 mM solution of sodium azide in 0.1 M KPi, at –0.2 V *vs.* RHE (ESI; Figure S14, series N_3RR-3). The ammonia concentration reaches values (> 200 µM) well above the experimental background (± 10 µM) after 4h of electrolysis, and there is a quasi-linear relationship between the total charge passed through the films and the quantity of ammonia produced as shown on Figure S15a (ESI). This strongly contrasts with the limited increase in NH_3 concentration (ca. 40 µM) measured after a 4h-long electrolysis run under similar conditions on bare glassy carbon electrode (ESI; Figure S14, series N_3RR-1). Importantly *a*-MoS_x did not demonstrate any intrinsic chemical reactivity towards azide leading to the release of ammonia in the electrolyte at room temperature, in the absence of an applied bias (ESI; Figure S14, series N_3RR-2). *a*-MoS_x thus, exhibits a clear activity for the electro-driven reduction of azide to ammonia.

In the enzymatic process the azide anion (N_3^-) is known to be reduced in a stoichiometric manner to ammonia and dinitrogen via an unusual two-electron three-proton transfer process, whereas hydrazoic acid (HN_3) reduction follows a six-electron six-proton pathway leading to the equimolar release of ammonia and hydrazine.[30] With a pKa of 4.6, hydrazoic acid (HN_3) accounts for about 16% of the azide species partition in our experimental conditions (pH 5.8) and we must consider both HN_3 and N_3^- as potential substrates for *a*-MoS_x. Only negligible amounts of hydrazine could be detected during the electrolysis (< 20 µM after 21h, ESI, Table S7) which suggests that the direct reduction of N_3^- is highly favoured on *a*-MoS_x over that of HN_3. This seems quite reasonable in view of the much stronger coordination to unsaturated Mo centers expected for the azide anion as compared to a neutral hydrazoic acid ligand. Considering an ideal two-electron reduction process, we can calculate an average FE of ca 50 ± 10% for azide reduction with a production rate of 3.5 ± 1.8 $mmol_{NH3}.h^{-1}mg_{\alpha\text{-}MoSx}^{-1}$ (or 29 ± 15 $mmol_{NH3}.h^{-1}Mo_{active}^{-1}$)[‡] from three distinct experiments. Since the accumulation of hydrazine is negligible in our experiments direct proton reduction best explain this limited FE.

The competitive production of hydrogen in these conditions was confirmed using gas chromatography analysis. For this, a pristine *a*-MoS_x film was polarized at –0.2 V vs. RHE for 6h, in 0.1 M KPi while continuously monitoring the quantity of hydrogen produced. After 2h of electrolysis 1 M sodium azide solution was added to reach a concentration of 10 mM at the cathode. It led to a sharp increase in the current density and a large drop in the production rate of hydrogen as shown on

Please do not adjust margins

Please do not adjust margins

Figure 3. Before addition of the azide in the electrolyte, the FE calculated for the hydrogen evolution reaction (HER) reaches about 70 ± 20% (t = 0 to 2h), whereas after the addition of NaN_3 the FE for HER sharply decreases to ca 2 ± 20% (t = 2h to 6h). Concomitantly a large quantity of ammonia is formed and a

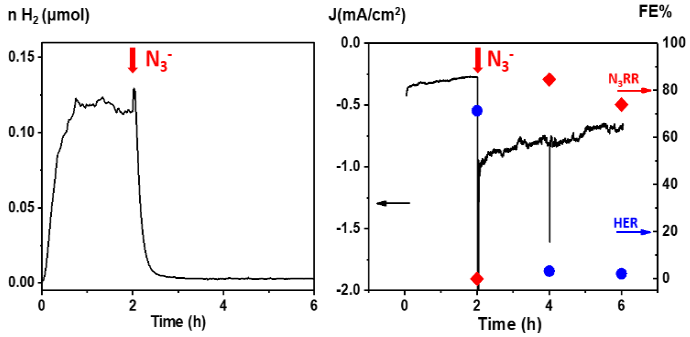

Figure 3: Real-time quantification of the hydrogen produced during a potential-controlled electrolysis in argon saturated 0.1 M potassium phosphate (pH = 5.8), using bare *a*-MoS_x film deposited on a GC electrode poised at -0.2 V *vs*. RHE (left). Evolution of the current density recorded during the electrolysis and point of faradic efficiencies for N_3^- reduction (N_3RR, red diamonds) and proton reduction (HER, blue dots; right). The red vertical arrows indicate the time of addition of a solution of 1 M NaN_3 in the cathode compartment (t = 2h, concentration reached at the cathode: 10 mM NaN_3).

concentration of 2.2 mM of NH_3 is measured at the end of the electrolysis (6h) corresponding to a minimum turnover number of 117 NH_3 per active Mo center.‡ It is worth noting that the FE of ammonia production calculated in the latter experiment (71%) is higher than the average FE (50 ± 10%) determined for electrolysis run in in the presence of 10 mM of azide from the beginning. This observation suggests a partial poisoning of the *a*-MoS_x catalytic sites by long term exposure to N_3^- ligand under non-catalytic conditions (no applied bias).

Despite having highlighted a partial Nitrogenase-like activity for *a*-MoS_x, this study demonstrates that the NRR activity is not intrinsic to all molybdenum sulfide derivatives, and that increasing the density of surface defects in these materials is not a universal strategy to enhance their activity towards NRR.

This work was supported by the French National Research Agency (ANR-15-IDEX-02, Labex ARCANE, CBH-EUR-GS, ANR-17-EURE-0003, and ANR-20-SODR-0004-03).

We are grateful to Adina Morozan, Jennifer Fize, Duc Nguyen Ngoc and Louis Dubrulle for their contributions to this work.

Conflicts of interest

There are no conflicts to declare.

Notes and references

‡ Estimation based on the mass ratio of Mo determined for *a*-MoS_x particles (36 wt%; ref. 22). Only Mo centers bearing terminal S_2^{2-} ligands are assumed to lead to active catalytic sites (Mo_{active}) under reductive conditions. For extended 1D coordination polymers of trigonal Mo clusters we count 1 active catalytic site (Mo_{active}) per $\{Mo_3S_7\}$ or $\{Mo_3S_6\}$ unit.

1 L. C. Seefeldt, Z.-Y. Yang, D. A. Lukoyanov, D. F. Harris, D. R. Dean, S. Raugei and B. M. Hoffman, *Chem. Rev.*, 2020, **120**, 5082.
2 A. J. Jasniewski, C. C. Lee, M. W. Ribbe and Y. Hu, *Chem. Rev.*, 2020, **120**, 5107.
3 Y. Abghoui, S. Sigtryggsson, E. Skùlason, *ChemSusChem* 2019, **12**, 4265
4 K. Tanaka, Y. Hozumi and T. Tanaka, *Chem. Lett.*, 1982, **11**, 1203.
5 A. Banerjee, B. D. Yuhas, E. A. Margulies, Y. Zhang, Y. Shim, M. R. Wasielewski and M. G. Kanatzidis, *J. Am. Chem. Soc.*, 2015, **137**, 2030.
6 J. Liu, M. S. Kelley, W. Wu, A. Banerjee, A. P. Douvalis, J. Wu, Y. Zhang, G. C. Schatz and M. G. Kanatzidis, *Proc. Natl. Acad. Sci.*, 2016, **113**, 5530.
7 L. M. Azofra, C. Sun, L. Cavallo and D. R. MacFarlane, *Chem. – Eur. J.*, 2017, **23**, 8275.
8 H. Guo, L. Li, X. Wang, G. Yao, H. Yu, Z. Tian, B. Li and L. Chen, *ACS Appl. Mater. Interfaces*, 2019, **11**, 36506.
9 J. Zhao, J. Zhao and Q. Cai, *Phys. Chem. Chem. Phys.*, 2018, **20**, 9248.
10 L. Zhang, X. Ji, X. Ren, Y. Ma, X. Shi, Z. Tian, A. M. Asiri, L. Chen, B. Tang and X. Sun, *Adv. Mater.*, 2018, **30**, 1800191.
11 X. Li, T. Li, Y. Ma, Q. Wei, W. Qiu, H. Guo, X. Shi, P. Zhang, A. M. Asiri, L. Chen, B. Tang and X. Sun, *Adv. Energy Mater.*, 2018, **8**, 1801357.
12 Y. Liu, M. Han, Q. Xiong, S. Zhang, C. Zhao, W. Gong, G. Wang, H. Zhang and H. Zhao, *Adv. Energy Mater.*, 2019, **9**, 1803935.
13 J. Zhang, X. Tian, M. Liu, H. Guo, J. Zhou, Q. Fang, Z. Liu, Q. Wu and J. Lou, *J. Am. Chem. Soc.*, 2019, **141**, 19269.
14 K. Chu, H. Nan, Q. Li, Y. Guo, Y. Tian and W. Liu, *J. Energy Chem.*, 2021, **53**, 132.
15 J. Wang, H. Nan, Y. Tian, and K. Chu, *ACS Sustainable Chem. Eng.* 2020, **8,** 12733.
16 X. Chen, Y.-T. Liu, C. Ma, J. Yub and B. Ding, *J. Mater. Chem. A*, 2019, **7**, 22235.
17 P. Wei, H. Xie, X. Zhu, R. Zhao, L. Ji, X. Tong, Y. Luo, G. Cui, Z. Wang, and X. Sun, ACS *Sustainable Chem. & Eng.* 2020, **8**, 29.
18 F. Lai, N. Chen, X. Ye, G. He, W. Zong, K. B. Holt, B. Pan, I. P. Parkin, T. Liu, and R. Chen *Adv. Funct. Mater.* 2020, **30**, 1907376.
19 P. D. Tran, M. Nguyen, S. S. Pramana, A. Bhattacharjee, S. Y. Chiam, J. Fize, M. J. Field, V. Artero, L. H. Wong, J. Loo and J. Barber, *Energy Environ. Sci.*, 2012, **5**, 8912.
20 T. Bourgeteau, D. Tondelier, B. Geffroy, R. Brisse, C. Laberty-Robert, S. Campidelli, R. de Bettignies, V. Artero, S. Palacin and B. Jousselme, *Energy Environ. Sci.*, 2013, **6**, 2706.
21 P. D. Tran, T. V. Tran, M. Orio, S. Torelli, Q. D. Truong, K. Nayuki, Y. Sasaki, S. Y. Chiam, R. Yi, I. Honma, J. Barber and V. Artero, *Nat. Mater.*, 2016, **15**, 640.
22 F. Xi, P. Bogdanoff, K. Harbauer, P. Plate, C. Höhn, J. Rappich, B. Wang, X. Han, R. van de Krol and S. Fiechter, *ACS Catal.*, 2019, **9**, 2368.
23 C. E. Bower and T. Holm-Hansen, *Can. J. Fish. Aquat. Sci.*, 1980, **37**, 794.
24 G. W. Watt and J. D. Chrisp, *Anal. Chem.*, 1952, **24**, 2006.
25 S. Z. Andersen, V. Čolić, S. Yang, J. A. Schwalbe, A. C. Nielander, J. M. McEnaney, K. Enemark-Rasmussen, J. G. Baker, A. R. Singh, B. A. Rohr, M. J. Statt, S. J. Blair, S. Mezzavilla, J. Kibsgaard, P. C. K. Vesborg, M. Cargnello, S. F. Bent, T. F. Jaramillo, I. E. L. Stephens, J. K. Nørskov, I. Chorkendorff, *Nature* **2019**, *570* (7762), 504–508.
26 I. Guevara, J. Iwanejko, A. Dembińska-Kieć, J. Pankiewicz, A. Wanat, P. Anna, I. Gołąbek, S. Bartuś, M. Malczewska-Malec and A. Szczudlik, *Clin. Chim. Acta*, 1998, **274**, 177.

 This journal is © The Royal Society of Chemistry 20xx

Please do not adjust margins

Please do not adjust margins

27 J. Choi, H.-L. Du, C. K. Nguyen, B. H. R. Suryanto, A. N. Simonov and D. R. MacFarlane, *ACS Energy Lett.*, 2020, **5**, 2095.
28 Th. Weber, J. C. Muijsers and J. W. Niemantsverdriet *J. Phys. Chem.* 1995, **99**, 9194.
29 R. D. Milton, S. Abdellaoui, N. Khadka, D. R. Dean, D. Leech, L. C. Seefeldt and S. D. Minteer, *Energy Environ. Sci*., 2016, **9**, 2550.
30 J. F. Rubinson, B. K. Burgess, J. L. Corbin and M. J. Dilworth, *Biochemistry*, 1985, **24**, 273.

This journal is © The Royal Society of Chemistry 20xx

Please do not adjust margins